

Flow Dynamics Near End-to-End Anastomoses Part II. Computer Flow Simulation

Y. H. Kim., Ph.D.

= Abstract =

A finite analytic(FA) numerical study was performed to determine flow dynamics in the vicinity of an end-to-end anastomosis. Experimental data of instantaneous lumen cross-section were used to simulate steady flow through an end-to-end anastomosis in order to solve the governing axisymmetric Navier-Stokes equations. Wall shear stresses increased proximal to the anastomosis in flow from the Penrose tubing to the PTFE graft. In flow the PTFE graft to the Penrose tubing, low wall shear stresses were observed distal to the anastomosis. The present study suggests a correlation between regions of low wall shear stress and the development of anastomotic neointimal fibrous hyperplasia(ANFH) in end-to-end anastomoses.

INTRODUCTION

Graft replacements in large arteries have been successful, the serious problem with loss of patency is encountered especially in medium and small diameter grafts less than 6mm in diameter[1]. Compliance mismatch between the host artery and the vascular graft is believed to be the most probable cause of graft failure[2-5]. It is possible that regions of compliance mismatch at the anastomosis may have abnormal flow dynamics, including increased wall shear stresses and regions of flow separation and stasis, which induce thrombus deposition. Abnormal flow dynamics, including increased wall shear stresses and regions of flow separation and stasis may exist in the vicinity of the anastomosis. Anastomotic neointimal fibrous hyperplasia(ANFH) is

a common occurrence after graft implantations, and it is most commonly seen around end-to-end anastomotic regions in all conduits[6,7].

Abnormal wall shear stress is believed by many investigators to be the principal fluid mechanical mediator of atherosclerosis[8-10]. Whether the abnormal flow pattern results directly from high or low shear stress on the arterial wall is still controversial. In order to elucidate the exact role of the wall shear stress in the development of the atherosclerotic plaques in arterial walls, a precise knowledge of hemodynamics in arteries is required. The purpose of this study is to investigate flow dynamics in the region of an end-to-end anastomosis due to the compliance mismatch between the host artery and the vascular graft using a finite analytic(FA) computational method.

<접수 : 1993년 1월 12일>

Cardiovascular Fluid Dynamics Laboratory, School of Chemical Engineering Georgia Institute of Technology, Atlanta, GA 30332-0100, U.S.A.

METHODS

The method to determine instantaneous geom-

etries in the anastomotic region of specimens under static loading is described elsewhere[11], and briefly introduced below. 6.35mm Penrose surgical drainage tubing was used to simulate an artery and was anastomosed with 6mm PTFE vascular grafts of two different thicknesses using a continuous suturing technique. Instantaneous diameters as a function of the distance from the anastomosis at each transmural pressure were used to simulate an axisymmetric laminar flow across an end-to-end anastomosis using the finite analytic(FA) method.

The FA method, developed by Chen and Chen [12], was employed for this numerical study. The basic idea of the FA method is the incorporation of a local analytic solution in the numerical solution of ordinary or partial differential equations. The local analytic solution with its local boundary values can be obtained by known analytic coefficients of the corresponding neighboring nodal values. This system of algebraic equations can be solved in conjunction with the boundary conditions of the problem to provide the FA numerical solution of the problem. Figure 1 shows the problem definition of the present numerical study with five different types of specimens. The flow from Penrose tubing to the PTFE graft simulated the proximal (upstream) anastomosis, while the flow from the PTFE graft to the Penrose tubing simulated the distal(downstream) anastomosis.

Typical boundary-fitted grid distributions for

corresponding flow configurations are shown in Figure 2. The number of grids in the radial direction was 15, and varied from 97 to 114 in the axial direction, depending on the problem geometry. Since the mean Reynolds number of the flow in the femoral arteries are approximately 250, $Re=250$ and 400 were chosen for this study. Parabolic, or uniform velocity profile was used for the upstream boundary condition, and a fully-developed flow was assumed for the downstream boundary condition. The dependence of the upstream boundary condition on the results was also analyzed. The continuity and momentum equations for incompressible laminar flow in cylindrical coordinates can be written as follows:

$$\text{Continuity equation: } \frac{\partial u}{\partial x} + \frac{\partial(rv)}{r\partial r} = 0 \quad (1)$$

Momentum equations in the axial direction:

$$\frac{Du}{Dt} = -\frac{\partial p}{\partial x} + \frac{1}{Re} \left[\frac{\partial^2 u}{\partial x^2} + \frac{1}{r} \frac{\partial}{\partial r} \left(r \frac{\partial u}{\partial r} \right) \right] \quad (2)$$

and in the radial direction:

$$\frac{Dv}{Dt} = -\frac{\partial p}{\partial r} + \frac{1}{Re} \left[\frac{\partial^2 v}{\partial x^2} + \frac{1}{r} \frac{\partial}{\partial r} \left(r \frac{\partial v}{\partial r} \right) \right] \quad (3)$$

$$\text{where } \frac{D}{Dt} = \frac{\partial}{\partial t} + u \frac{\partial}{\partial x} + v \frac{\partial}{\partial r} \quad (4)$$

The one-velocity staggered-grid system was used such that the velocity components and the pressure are calculated at different nodes, but stored as values of the same grid in the computer. The Patankar's SIMPLER method was employed in the solution procedure so that velocity field could be updated after obtaining the pressure correction with the continuity equation.

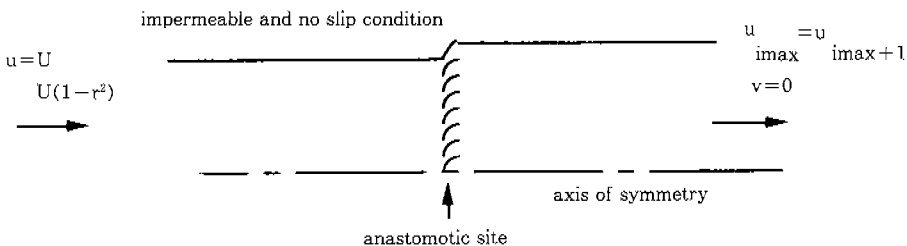


Fig. 1 Flow configuration of the present study.

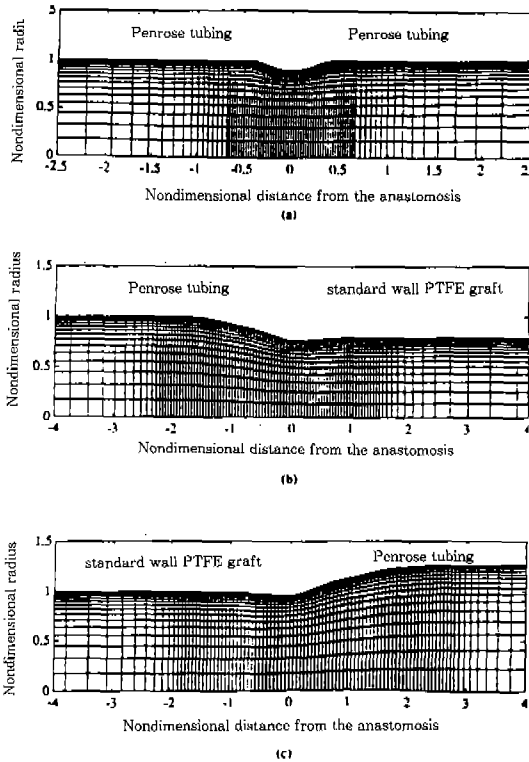
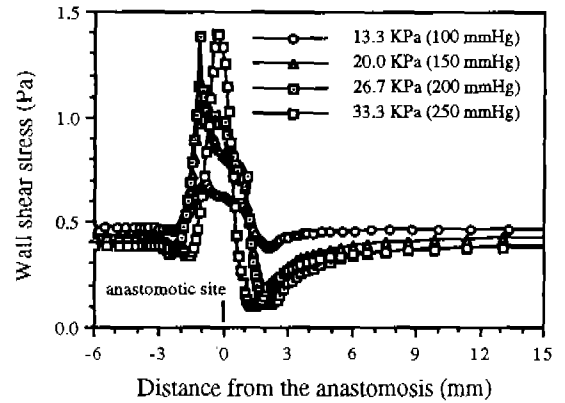


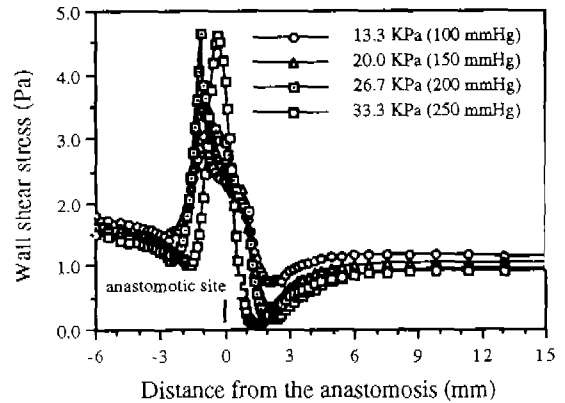
Fig. 2 Mesh distributions used for flow simulations.
 (a) Artery-artery junction.
 (b) Proximal anastomosis.
 (c) Distal anastomosis.

RESULTS

The wall shear stress distribution across the Penrose tubing-Penrose tubing anastomosis, simulating an artery-artery junction, at various transmural pressures for $Re=250$, with parabolic and uniform inlet velocity profile, is shown in Figure 3. The computed wall shear stress far from the anastomotic site was in close agreement with magnitudes computed from the Poiseuille flow solutions. However, large changes in the wall shear stress were found near the anastomotic region. High wall shear stresses were computed proximal to the suture line, and low wall shear stresses were found distally. For flow through the Penrose tubing-Penrose tubing anastomosis, a flow separation



(a)



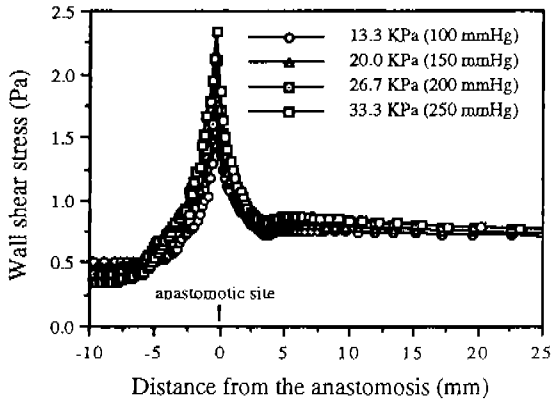
(b)

Fig. 3 Wall shear stress distribution at $Re=250$ for a Penrose tubing-Penrose tubing anastomosis.

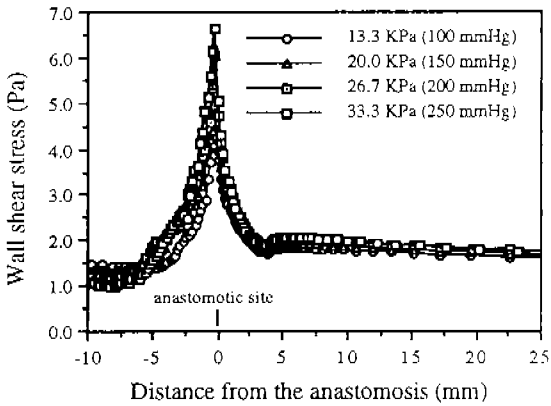
- (a) With parabolic inlet velocity profile.
 (b) With uniform inlet velocity profile.

was observed about 2mm distal to the anastomotic site at higher transmural pressures with uniform flow inlet boundary condition.

Figure 4 shows the wall shear stress distribution in flow from the Penrose tubing to standard wall graft (proximal or upstream anastomosis) at $Re=250$, with various transmural pressures and inlet velocity conditions. As the transmural pressure increased, increased shear stresses were found on the Penrose tubing side very near the suture line. With uniform velocity condition at the upstream, the same trend was found except that the magnitudes of wall shear



(a)



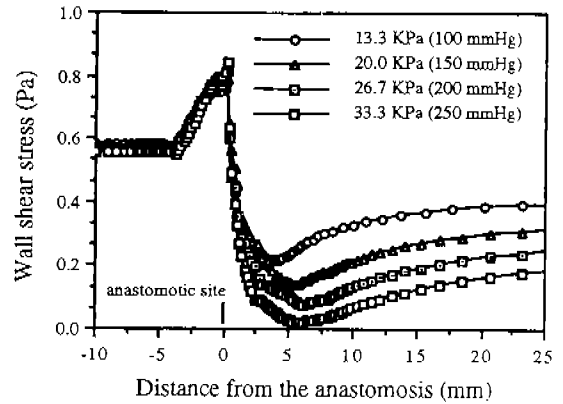
(b)

Fig. 4 Wall shear stress distribution at $Re=250$ for a Penrose tubing-standard wall graft anastomosis (proximal anastomosis).

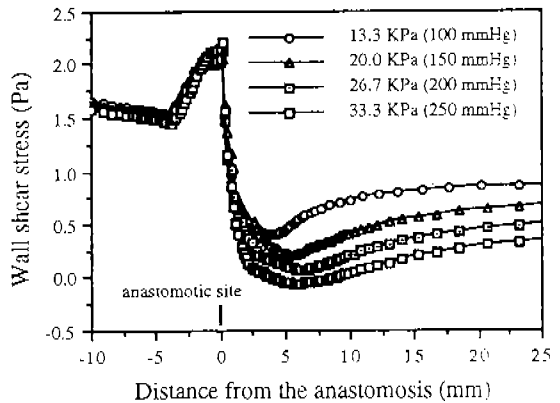
- (a) With parabolic inlet velocity profile.
- (b) With uniform inlet velocity profile.

stresses were larger than in the previous case.

Wall shear stress distributions in flow from the standard wall graft to Penrose tubing (distal or downstream anastomosis) at the same Reynolds numbers are shown in Figure 5. In this case, the significant decrease of the wall shear stress was observed at about 6mm distal to the anastomosis in the Penrose tubing. The indication of flow separation was observed at 3.9mm downstream of the anastomosis with standard wall graft-Penrose tubing anastomosis at trans-



(a)



(b)

Fig. 5 Wall shear stress distribution at $Re=250$ for a standard wall wall graft-Penrose tubing anastomosis (distal anastomosis).

- (a) With parabolic inlet velocity profile.
- (b) With uniform inlet velocity profile.

mural pressure of 250mmHg with uniform inlet velocity condition, and the laminar reattachment occurred at 8.9mm downstream of the anastomosis.

Very similar trends were observed with thin wall PTFE graft anastomosis compared with standard wall graft. However, the region of abnormally high or low shear stress was located nearer to the anastomotic site with thin wall grafts than that with standard wall thickness grafts. Figure 6(a) and 6(b) compare the wall

Table 1 The maximum and minimum wall shear stress of Penrose tubing-Penrose tubing anastomosis at various transmural pressures.

unit = Pa

Re	upstream condition	13.3KPa (100mmHg)		20.0KPa (150mmHg)		26.7KPa (200mmHg)		33.3KPa (250mmHg)	
		max.	min.	max.	min.	max.	min.	max.	min.
250	parabolic	0.68 (-0.9)	0.37 (2.0)	1.09 (-0.9)	0.18 (2.1)	1.38 (-1.1)	0.11 (2.1)	1.40 (-0.3)	0.10 (1.4)
	uniform	3.18 (-1.0)	0.70 (2.1)	3.87 (-1.0)	0.28 (2.1)	5.03 (-1.1)	0.08 (2.1)	4.87 (-0.3)	-0.02 (1.4)
400	parabolic	1.60 (-1.0)	0.44 (2.1)	1.97 (-1.0)	0.22 (2.1)	2.51 (-1.1)	0.11 (2.1)	2.46 (-0.3)	0.07 (1.4)
	uniform	6.26 (-1.0)	0.77 (2.1)	7.78 (-1.0)	0.21 (2.1)	10.31 (-1.1)	-0.15 (2.1)	9.93 (-0.3)	-0.34 (1.4)

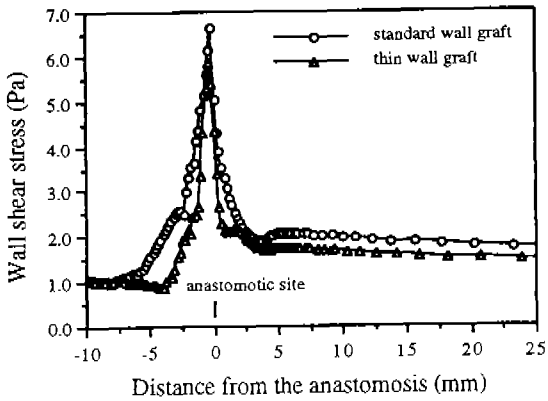
Note : The numbers in parenthesis specify the distance from the anastomosis(mm).

Table 2 The maximum and minimum wall shear stress in the vicinity of Penrose tubing-PTFE vascular graft anastomosis at various transmural pressures.

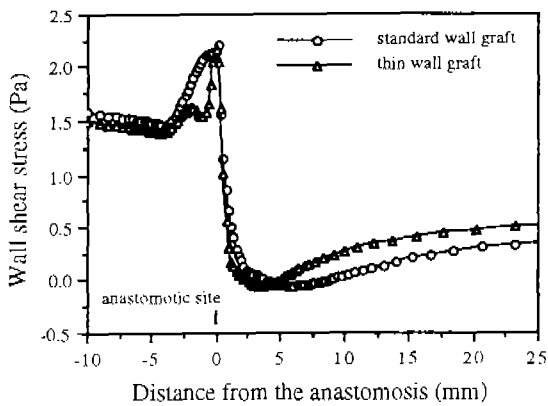
unit = Pa

Re 250	upstream condition	13.3KPa (100mmHg)		20.0KPa (150mmHg)		26.7KPa (200mmHg)		33.3KPa (250mmHg)	
		max.	min.	max.	min.	max.	min.	max.	min.
Flow from Penrose tubing to standard wall graft	Parabolic	1.65 (-0.2)	0.72 (3.9)	1.69 (-0.2)	0.76 (4.1)	2.11 (-0.2)	0.80 (3.9)	2.33 (-0.2)	0.82 (3.8)
	uniform	4.74 (-0.2)	1.71 (3.9)	4.76 (-0.2)	1.79 (4.1)	6.04 (-0.2)	1.89 (3.9)	6.65 (-0.2)	1.89 (3.7)
Flow from Penrose tubing to thin wall graft	parabolic	0.78 (-0.8)	0.55 (4.0)	1.20 (-0.4)	0.62 (4.0)	1.60 (-0.4)	0.68 (4.0)	1.94 (-0.4)	0.71 (4.1)
	uniform	2.14 (-0.8)	1.34 (4.0)	3.46 (-0.4)	1.51 (4.0)	4.76 (-0.4)	1.66 (4.0)	5.87 (-0.4)	1.71 (4.1)
Flow from standard wall graft to Penrose tubing	Parabolic	0.81 (0.2)	0.21 (4.2)	0.53 (0.2)	0.14 (5.8)	0.82 (0.2)	0.07 (6.2)	0.84 (0.2)	0.02 (6.0)
	uniform	2.13 (0.2)	0.39 (4.2)	2.05 (0.2)	0.21 (5.7)	2.13 (0.2)	0.06 (6.2)	2.21 (0.2)	-0.06 (5.8)
Flow form thin wall graft to Penrose tubing	Parabolic	0.71 (0.2)	0.20 (3.7)	0.72 (0.0)	0.21 (3.2)	0.76 (0.0)	0.11 (3.4)	0.80 (0.0)	0.02 (3.8)
	uniform	1.96 (0.2)	0.36 (3.7)	1.92 (0.0)	0.41 (3.2)	2.05 (0.0)	0.14 (3.4)	2.17 (0.0)	-0.06 (3.6)

Note : The numbers in parenthesis specify the distance from the anastomosis(mm).



(a)



(b)

Fig. 6 Comparison of wall shear stress distribution between standard and thin wall vascular grafts anastomosed to Penrose tubing at $Re=250$ with uniform inlet velocity profile.

shear stress distribution across the anastomosis with standard and thin wall grafts. Table 1 and 2 show the maximum and the minimum values of the wall shear stress, with their locations, across penrose tubing-Penrose tubing and standard wall as well as thin wall graft anastomosis respectively.

DISCUSSION

For flow from the Penrose tubing to PTFE vascular grafts simulating the proximal or up-

stream junction, increased wall shear stress was observed in both experimental and numerical studies. On the other hand, for flow the Penrose tubing to PTFE grafts, simulating the distal or downstream anastomosis, decreased wall shear stress was observed distal to the anastomosis. Wall shear stresses obtained in this study are comparable to the mean shear stresses reported for the femoral arteries of 1.4-1.6 Pa[13,14]. Rodgers et al.[15] theoretically computed the mechanical shear stress distribution at an end-to-end anastomosis with a continuous suture. The point of separation of about 2mm distal to the Penrose tubing-Penrose tubing anastomosis in the present study was in agreement with their results with carotid artery anastomoses. The wall shear stress was also found to be higher at the proximal position of the suture line, which agrees well with the present study. In flow from the Penrose tubing to the vascular graft, larger magnitudes of wall shear stress were located proximal to the anastomotic site. Chandran et al.[16] demonstrated a region of high-stress concentration on the graft side just near the anastomosis using a finite element analysis. Fry[9] examined the influence of wall shear stress levels on the integrity of endothelium and suggested that deformation, swelling and eventual erosion of the endothelium may occur at sites where the local wall shear stress is relatively high. His study suggested that exposure of the endothelial surface to a time-averaged wall shear stress of approximately 38 Pa would result in remarkable deterioration of the endothelial surface. Brown et al.[17] have shown that platelet lysis takes place at a shear stress of the order of 10-15 Pa. The maximum wall shear stress from the present steady flow simulation was 6.65 Pa at $Re=250$, which is high enough to create platelet lysis.

Magnitudes of wall shear stress were signifi-

cantly smaller distal to the anastomotic site in flow from the prosthetic graft to the Penrose tubing. Caro et al.[10] found that early atherosclerosis tended to develop predominantly in regions of low wall shear stress. Their hypothesis is based on a series of events which lead to a shear-dependent diffusional efflux of cholesterol from the intima to the bloodstream. Rittgers et al.[18], using a hot film anemometer, supported this hypothesis due to the fact that greater intimal plaques were formed at regions of low shear stress. The present steady FA flow simulations revealed a flow separation distal to the PTFE graft-Penrose tubing anastomosis. Incidences of hyperplasia have been found to be greater at the distal or downstream anastomosis[6,7,19], where low wall shear stresses were computed in the present study. Hence, a correlation between low wall shear stress and anastomotic hyperplasia is suggested from the results. The nonlinear characteristics of the wall shear stress with respect to the Reynolds number is noted at distal positions of the anastomosis in this type of flow. It also suggests that the increased flow rate may not provide a wash-out of other fluid in this low shear stress region. The compliance mismatch across the anastomotic site creates an abnormal geometry near the anastomosis, which might result in a very high shear stress near the anastomosis or a flow separation distal to the anastomosis.

The main factor which governs the hemodynamics across the anastomosis might be the lumen geometry subject to the transmural pressure instead of the fluid dynamic properties such as Reynolds number. Therefore, it can be said that, patients with hypertension may have more severe intimal hyperplasia. The abnormally high shear stress at the anastomotic site might damage the endothelial layer to create the atherosclerosis or the graft failure in this re-

gion. On the other hand, regions of low shear stress at the distal anastomosis have been shown to be preferential locations for ANFH. The diameter of the vascular graft is often chosen to be slightly larger than that of the host artery based on the fact that the compliance of the vascular grafts is much smaller than that of the host arteries. In this case, lumen geometry can be worse than that in the anastomosis with vascular grafts of the same diameter. In the physiological pulsatile flow, the instantaneous lumen geometry would be strongly more dependent on the transmural pressure. Then, the low shear distal to the graft-artery anastomosis (downstream anastomosis) would be much more critical. Local flow separation might also have a causal effect on ANFH development. Recently, Giddens et al.[20] claimed that the determining factor of the intimal hyperplasia may be the maximum wall shear experienced during the cycle regardless of directions and not simply the mean shear rate. On the contrary, with a high transmural pressure the high shear stress will be observed just proximal to the artery-graft anastomosis (proximal or upstream anastomosis). Binns et al.[21] suggested that an optimal graft diameter may contribute to the prevention of neointimal hyperplasia and pseudointimal thickening by optimizing shear stress to near normal levels. Flow separation and increased shear stresses are possible causes of endothelial cell injury, and subsequent platelet and white cell deposition.

The present study did not incorporate all of the physiological conditions of the human body. Specifically, the flow simulation utilized steady flow, a Newtonian fluid, axisymmetric geometry, and a rigid wall at each pressure level. The human cardiovascular system, on the other hand, is characterized by pulsatile flow, a non-Newtonian fluid and visco-elastic properties of

vessels. The hemodynamics at an anastomosis also depend on the type, shape and size of the anastomosis, diameter of structures anastomosed and the suturing material and technique [19,22]. Despite these limitations, the numerical results do provide valuable insight into the hemodynamic characteristics that could occur clinically in the vicinity of an anastomosis.

CONCLUSIONS

A finite analytic(FA) numerical study was performed to determine the flow dynamics in the vicinity of end-to-end anastomoses using the experimentally measured instantaneous lumen cross sections. From the present study, the following conclusions can be drawn:

1. The wall shear stress increased just proximal to the Penrose tubing-Penrose tubing anastomosis(simulating an artery-artery anastomosis), and decreased to magnitude smaller than the normal wall shear stress. A region of flow separation was observed at about 2mm distal to the Penrose tubing-Penrose tubing anastomosis(simulating an artery-artery anastomosis) at higher transmural pressures.
2. In Flow from the Penrose tubing to PTFE grafts, simulating the upstream junction, the maximum wall shear stress was computed proximal to the anastomosis. With higher flow rate due to exercises, the results indicated that the wall shear stress might be very close to 40 Pa, the critical shear for damaging the endothelial layer that Fry[9] reported early.
3. The region of abnormally increased or decreased wall shear stress is located nearer to the anastomotic site for flow with the thin wall vascular graft anastomosis than with the standard wall vascular graft anastomosis.

4. In flow from the vascular graft to the Penrose tubing, simulating the downstream anastomosis, the minimum wall shear stress was computed distal to the anastomosis.
5. The region of low shear stress in flow from PTFE grafts to the Penrose tubing was located closer to the anastomosis with thin wall grafts than that with standard wall thickness grafts.
6. The wall shear stress distribution was found to be dependent upon the specified inlet velocity distribution with magnitudes of wall shear stress being larger with a flat inlet velocity profile. In flow from the vascular graft to the Penrose tubing with a flat inlet velocity profile, a flow separation was observed distal to the anastomosis at higher transmural pressures. Since the flow in the peripheral vessels is not expected to be fully developed, a flat inlet velocity profile may be more realistic for the analysis.

In conclusion, the present study clearly revealed that the compliance mismatch across the anastomosis is the main factor in abnormal fluid dynamics. The compliance should be considered as an important design characteristics in order to reduce flow induced shear stress on platelets and endothelial cells, anastomotic stress and energy dissipation.

REFERENCES

- 1) Hunter, T.J.; Schmidt, S.P.; Sharp, W.V.; Malindzak, G.S. "Controlled Flow Studies in 4mm Endothelialized Dacron Grafts", *Trans. Am. Soc. Artif. Intern. Organs* 29: 177-182, 1983
- 2) Abbott W.M.; Bouchier-Hayes D.J. "The Role of Mechanical Properties in Graft Design" in *Graft materials in vascular surgery* H.Dordich Eds., Chicago, pp.59-78, 1981

- 3) Abbott, W.M.; Megerman, Hasson, J.E.; L' Italien, G.; Warnock, D.F. "Effect of Compliance Mismatch on Vascular Graft Pathency", *J. Vasc. Surg.* 5:376-382, 1985
- 4) Clark, R.E.; Apostdou, S.; Kardos, J.L. "Mismatch of Mechanical Properties as a Cause of Arterial Prostheses Thrombosis", *Surg. Forum* 27:208-210, 1976
- 5) Imparato, A.M.; Bracco, A. "Intimal and Neointimal Fibrous Proliferation Causing Failure of Arterial Reconstructions", *Surg.* 72:1007-1017, 1972
- 6) LoGerfo, F.W.; Quist, W.C.; Nowak, M.D. "Downstream Anastomotic Hyperplasia: A Mechanism of Failure in Dacron Arterial Grafts", *Ann. Surg.* 197:479-483, 1983
- 7) LoGerfo, F.W.; Soncrant, T.; Teel, T.; Dewey, C.F. "Boundary Layer Separation in Models of Side-to-End Arterial Anastomoses", *Arch. Surg.* 114:1369-1373, 1979
- 8) Caro C.G. "Transport of Material Between Blood and Wall in Arteries" in *Atherosclerosis: Initiating Factors*, A Ciba Foundation Symposium 12, pp.127-164, 1973
- 9) Fry, D.L. "Response of the Arterial Wall to Certain Physical Factors" in *Atherosclerosis: Initiating Factors*, A Ciba Foundation Symposium 12, pp.93-126, 1973.
- 10) Morinaga, K.; Okadome, K.; Kuroki, M.; Miyazaki, T.; Muto, Y.; Inokuchi, K. "Effect of Wall Shear Stress on Intimal Thickening of Arterially Transplanted Autogenous Veins Dogs", *J.Vasc. Surg.* 2:430-433, 1985
- 11) Kim, Y.H.; Chandran, K.B.; Bower, T.J.; Corson, J.D. "Fluid Dynamics in the Vicinity of an End-to-End Anatomosis and ITS Relationship with the Anastomotic Neointimal Fibrous Hyoperplasia", *Advances in Bioengineering*, pp.243-246, 1991.
- 12) Chen, C.J.; Chen, H.C. "Finite Analytic Numerical Method for Unsteady Two-Dimensional Navier-Stokes Equations", *J.Comp. Phys.* 53:209-226, 1984.
- 13) Johnson, G.A.; Hung, J-K.; Brant, A.M.; Borovetz, H.S. "Experimental Determination of Wall Shear Rate in Canine Carotid Arteries Perfused In Vitro", *J.Biomech.* 22: 1141-1150, 1989
- 14) Kamiya, A.; Togawa, T. "Adaptive Regulation of Wall Shear Stress to Flow Change in the Canine Carotid Artery", *Am. J. Physiol.* 239:H14-18, 1980.
- 15) Rodgers, V.G.J.; Teodori, M.F.; Borovetz, H.S. "Experimental Determination of Mechanical Shear Stress about an Anastomotic Junction", *J.Biomech.* 20:795-803, 1987
- 16) Chandran, K.B.; Gao, D.; Han, G.; Baraniewski, H.; Corson, J.D. "A Finite Element Analysis of Artery-Graft Anastomosis", *Medical and Biological Engineering and Computing* (In press), 1991.
- 17) Brown, C.H.; Leverett, L.B.; Lewis, C.W. "Morphological, Biochemical and Functional Changes in Human Platelets Subjected to Shear Stresses", *J.Lab Clin. Med.* 86:462-471, 1971
- 18) Rittgers, S.E.; Karayannacos, P.E.; Guy, J. F.; Nerem, R.M.; Shaw, G.M.; Hostetler, J.R.; Vasco, J.S. "Velocity Distribution and Intimal Proliferation in Autolous Vein Grafts in Dogs", *Circ. Res.* 42:792-801, 1978.
- 19) Hasson, J.E.; Megerman, J.; Abbott, W.M. "Suture Technique and Perianastomotic Compliance", *J.Vasc. Surg.* 3:591, 1986.
- 20) Giddens, D.P.; Zarins, C.K.; Giddens, E. M.; Bassiouny, H.; Glagov, S. "Exercise Flow Affects Hemodynamics of End-to-Side Vascular Models", *Proceedings 3rd.*

- USA-China-Japan Conference on Bio-mechanics, pp.66-67, 1991.
- 21) Binns, R.L.; Ku, D.N.; Stewart, M.T.; Ansley, J.P.; Coyle, K.A. "Optimal Graft Diameter: Effect of Wall Shear Stress on Vascular Healing", *J. Vasc. Surg.* 10:326-337, 1989.
- 22) Kinley, C.E.; Paasche, P.E.; MacDonald, A.S.; Marble, A.E.; Gozna, E.R. "Stress at Vascular Anastomosis in Relation to Host Artery: Synthetic Graft Diameter", *Can J. Surg.* 17:74-76, 1974.